UNIVERSITY OF TWENTE.

FERROELECTRIC PROPERTIES AROUND THE MPB OF $\mathrm{PbZr_{1-x}Ti_xO_3}$ THIN FILMS

Bachelor Thesis

at Inorganic Material Science

Supervisors:
Gertjan Koster
Nirupam Banerjee
Xin Wan

Author:
Daniel Zschocke

May 2, 2012

Contents

1 Introduction

Although the energy demand decreased in 2009, in 2010 the world-wide energy consumption rose by 5% [1]. Predictions also assume a fast growing demand in the future. Neglecting the big environmental issues caused by fossil energy sources, they also will deplete in the upcoming decades. Till then there must be an sustainable solution. Regarding that new energy sources depend greatly on the circumstances you will need a broad variety of sustainable energy sources. One component to that wide field of energy systems could be the research in thin films of lead zirconate titanate(PZT); $PbZr_{1-x}Ti_xO_3$. The properties of this ferroelectric material in bulk phase are known to be outstanding. In a thin film PZT I expect that the switching of the polarization is more easily achieved, because the structure of the material does arrange in a coexistence of rhombohedral and tetragonal structure around the morphotropic phase boundary at $x = 0.52$. In my investigations I will make samples of PZT of different compositions around the morphotropic phase boundary by pulse laser deposition. I will use X-ray diffraction to measure the crystalinity. To measure the ferroelectricity the ferroelectric tester will be used. The facts provided by this thesis can serve as a reference for future research in PZT thin films to develop sustainable energy materials.

2 Fundamentals of bulk lead zirconate titanate

Lead zirconate titanate (PZT)[1] has the chemical formula $Pb[Zr_{1\text{-}x}Ti_x]O_3$ and is an inorganic compound. This ceramic perovskite possesses considerable piezoelectric and ferroelectric properties notably at the morphotropic phase boundary region[2]. This is the region where the crystal structure arranges in a monoclinic phase therefore enhancing the polarization possibilities of the material and as a result providing this high piezoelectric effect[3]. It is worthwhile to consider first the fundamental properties of PZT, such as crystal structure, ferroelectricity and piezoelectricity, to understand how it comes to this high piezoelectric constant.

2.1 Crystal structure

PZT arranges in a crystal with lead atoms in the corners, oxygen atoms on the planes and either zirconate or titanate in the centre. Depending on the stoichiometric composition the crystal structure is either tetragonal or rhombohedral[2](figure 1).

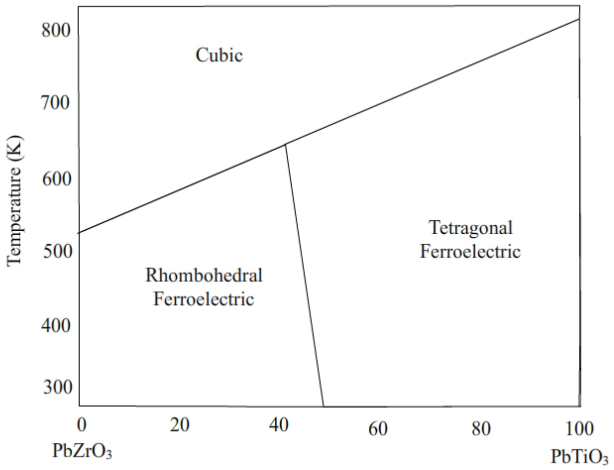

Figure 1: A simplified phase diagram of PZT showing the crystal structure depending on composition and temperature [4]

---

[1] Lead zirconate titanate will be abbreviated with PZT throughout the text

[2] PZT can also arrange in a cubic structure, but only above the Curie-Temperature

Apart from this there exist a narrow region in between those two crystal structures which is called the morphotropic phase boundary. This is where the material has astounding ferroelectric and piezoelectric properties[3].

A composition of more titanate than zirconate results in a tetragonal crystal structure(figure 2a) on the contrary a composition of more titanate than zirconate results in a rhombohedral crystal structure(figure 2b).


(a)

(b)

Figure 2: The crystal structure of PZT (The purple spheres are lead, the red spheres are oxygen and the small blue sphere is either titanium or zirconate) a) tetragonal and b) rhombohedral

The centre atom zirconate or titanate is not in the symmetrical centre but shifted a bit. As a consequence the charge distribution is not any more evenly spread but shifted. This leads to a formation of dipoles, what in particular is compulsory for ferroelectric materials.

2.2 Ferroelectricity

Ferroelectric materials are insulating materials which can undergo “spontaneous” polarization. This means that there are stable states of electric polarization with no electric field applied. Materials which consist of dipoles can experience polarization because usually the dipoles are not arranged in an ordered manner, by applying an external electric field the dipoles try to align to the electric field(figure 3).

Polarization is best described by a graph showing the polarization versus the applied electric field. Depending on the material the graph looks different, however three main shapes can be observed. In figure 4 those three shapes are illustrated.

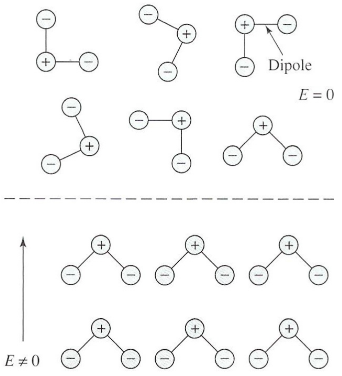

Figure 3: Dipoles getting arranged by an external electric field[5]

When a material exhibits one of those shapes it has a dielectric, paralectric or ferroelectric polarization.

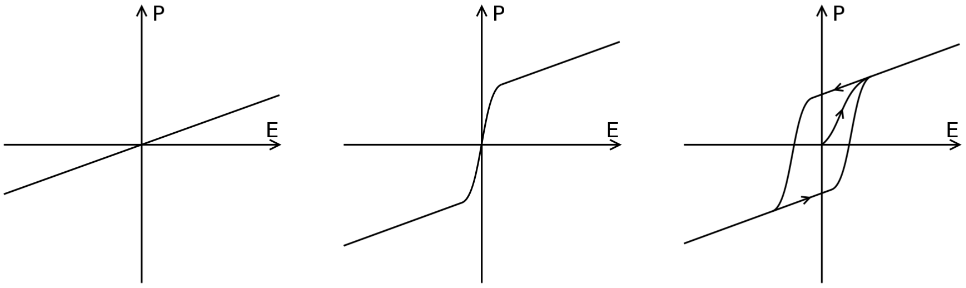

(a) Dielectric Polarization

(b) Paraelectric Polarization

(c) Ferroelectric Polarization

Figure 4: Different forms of electric materials classified by Polarization to electric field behaviour; a) shows a linear relation and is called dielectric polarization, b) shows strong and a weak linear relation, paralectric polarization and c) shows a hysteretic relation, ferroelectric polarization [6]

Compared to the other two, with ferroelectric materials the polarization is still present when the electric field has been removed. Furthermore, after applying once an electric field the polarization is permanent and can only be brought to zero by a permanent application of an electric field. Moreover, the polarization can be switched by a contrary electric field and vice versa. This loop is called hysteresis. In figure 5 a more detailed hysteresis loop can be seen. Of special interest is the remanent polarization which is indicated by P_r. It is the polarization remaining when the electric field is removed. The coercive field strength E_c which is shown in figure 5 is the electric field strength needed to achieve a polarization of zero.

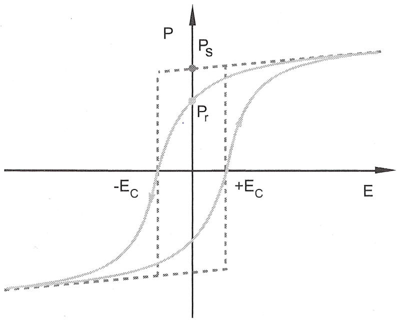

Figure 5: Hysteresis loop of polycrystalline sample (full line) and single domain single crystal (dashed line) [7]

PZT has such a good ferroelectric property, which can be explained by a closer look at the structure. In the tetragonal phase(Ti rich) the centre ion is a bit displaced to one of the six cell faces, due to the attraction of the O ion. All six shift directions are identical, regarding the free energy and so equally possible. The same is observed for the rhombohedral phase (Zr rich). In spite of a shift to the cell faces a shift towards the eight cell corners is observed. As in section 2.1 already stated these shifts lead to creation of dipoles and consequently forming polarization directions. In brief, the tetragonal and rhombohedral structure have six and eight polarization possibilities. Near the morphotropic phase boundary, where both phases coexist, up to $6 + 8 = 14$ polarizations are possible. This means that a polarization switch can be achieved more readily, hence there are more intermediate steps to overcome the needed energy maximum[8].

In figure 5 two hysteresis loops can be seen; the dashed line indicates a single domain single crystal and the full line a polycrystalline ferroelectric hysteresis loop. This is because in a single domain single crystal all polarization vectors of each unit cell point into the same direction when an electric field of enough strength is applied, if the field is to low no switching will occur. That is why the polarization spontaneous switches. In a polycrystalline material there are domains of same polarization. These are small volumes where each polarization vector points into the same direction within this small volume. Through the polycrystalinity different domains with different orientations exist which switch polarization at different electric field strengths. Due to this the shape of the hysteresis loop is rounder.

3 Sample fabrication and characterization

The following section will outline how the samples were made and which measurements were used to determine the properties.

3.1 Sample fabrication

The samples were deposited by pulsed laser deposition (PLD) a powerful technique to make thin film materials. This technique uses high power laser pulses to vaporize, melt and ionize the hardest and most heat resistant materials from a target. When the laser hits the target material a plasma plume is generated which expands away from the target to a substrate and condenses on it. Secondly, for measurement purposes, the samples were structured to form capacitors by photo-lithography.

3.1.1 Experimental Setup

The setup of a PLD-system is shown in figure 6. At the bottom right the laser beam passes through a focussing lens before entering the vacuum chamber through a quartz window. Inside the vacuum chamber the laser beam hits the rotating target material. The material gets ablated by irradiation and a luminous cloud can be seen, which is called ‘plume’. This plume transfers the material to the substrate.

The advantages of PLD compared to other deposition methods are the following[10]:

- Deposition of materials with high melting points such as PZT
- Low contamination of sample
- Stoichiometric deposition

Especially that the target composition can be deposited on the substrate is a crucial fact. Apart from this low contamination is required, leading to a consistent crystal structure of the sample. In the following the single parts of the PLD-system are explained in more details.

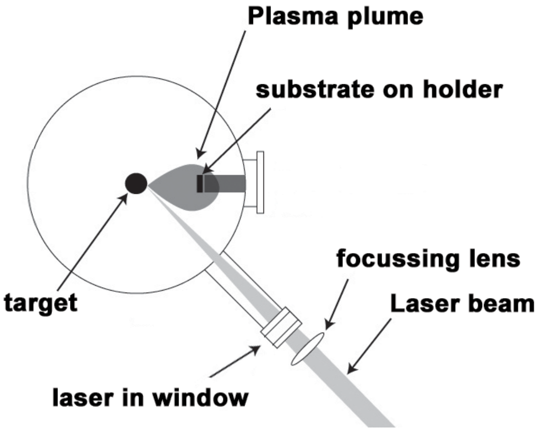

Figure 6: Schematic view of a PLD-system [9]

The Exciplex Laser

In this study a KrF exciplex laser at a wavelength of $\lambda = 248$nm and a pulse duration of 25ns is used. The pulse energy density which will be emitted on the target can range from 1–5J cm^{-2} and the repetition rate from 1–50Hz. A mask is used to achieve a better homogeneous energy density[11]. Before the lase beam hits the target in a 45° angle to the target normal it is focused by a lens. By adjusting the mask and lens position the spot size can be modified.

Substrate

The ablated material from the target will deposit on a substrate. The purpose of the substrate is to have a good base on which the deposition can be executed. The first atom layers of the deposited material will adopt the crystal structure of the subjacent substrate and as a consequence this leads to a more epitaxial growth. Strontium Titanate (STO) in the configuration (001) was the substrate of choice. This is because the thereon growing PZT will also align in a (001) configuration leading to high ferroelectric properties.[12] The substrate size is 5 x 5 mm^2. Before deposition ultra sonic cleaning of the substrates in acetone and ethanol was executed. Furthermore, the substrates were annealed for 2 h at 950 °C.

Targets

The bulk materials, which is ablated by the laser and therefore is deposited as a thin film on the substrate, are called Targets. They are shaped in cylindrical form and attached to a holder, so that they can turn around the cylinder axis while deposition. This is to achieve an evenly penetration by the laser. To deposit electrode layers a $SrRuO_3$ target has been used. Why electrode layers are needed is outlined in section 3.1.2. SRO has the advantage that it has a high chemical and structural similarity with PZT as well as STO and consequently leading to a epitaxial growth[13].

Overall six samples have been made, all with different PZT compositions(table 1). The compositions lie around the morphotropic phase boundary with a 3% spacing between compositions, this is to guarantee a thoroughly determination of the investigated properties around the MPB.

Name	PZT_1	PZT_2	PZT_3	PZT_4	PZT_5	PZT_6
Composition (Zr/Ti)	58/42	55/45	52/48	49/51	46/54	43/57

Table 1: Investigated PZT compositions

The vacuum chamber

The used vacuum chamber can reach a base pressure of $10^{-6} - 10^{-7}$mbar. However during deposition the pressure can be adjusted in the range of $10^{-3} - 10^{0}$mbar by the flow rate of oxygen which serves as deposition gas. The oxygen gas serves also to guarantee a stoichiometric growth, because the oxygen ions which were ablated from the target have a lower velocity than the other materials, which leads to a lack of oxygen atoms at the substrate surface. Therefore, the oxygen flow compensates this lack and provides enough oxygen for the oxidation reaction. In addition, the higher pressure slows down the ablated ions and thereby prevents them to penetrate the substrate.[14]

3.1.2 Fabrication process

For ferroelectric and piezoelectric measurement purposes the samples were fabricated in a way that they form a capacitor. SRO serves as electrode material which is separated by PZT being the insulator material. To achieve such a structure, the samples were grown as indicated in figure 7. First the SRO bottom electrode, next PZT and finally again SRO as top electrode was deposited.

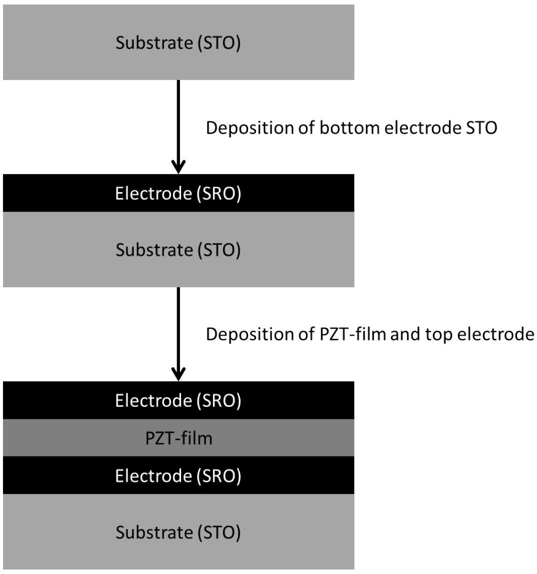

Figure 7: Schematic of fabrication process

The used grow parameters per target are shown in table 2. SRO was deposited for 20 minutes resulting in a thickness of 100 nm and PZT for 9 minutes resulting in a thickness of 250 nm.

3.1.3 Structuring process

Through the fabrication process the layers are already arranged in the order of a capacitor, but it is not possible to measure the bottom-electrode, hence it is between the substrate and the ferroelectric. In order to create a measurable capacitor it is needed to structure the samples. In this study a top-to-top electrode structure was applied. In other words, two capacitors in series will be used, one from the top electrode to the bottom electrode and a second through the bottom electrode to

Parameter	$SrRuO_3$(SRO)	$Pb(Zr_xTi_{1-x})O_3$(PZT)
Mask	1 hole ($56.5mm^2$)	1 rectangle ($98mm^2$)
Energy density ($J\,cm^{-2}$)	2.5	3.5
Spot size (mm^2)	1.9	3.0
Laser pulse frequency (Hz)	4	10
Ambient pressure (mbar)	0.13 (O_2)	0.10 (O_2)
Target-to-substrate distance (mm)	49	60
Deposition temperature (°C)	600	600
Deposition rate ($nm\,pulse^{-1}$)	0.022	0.042

Table 2: Thin film grow parameters for SRO and PZT

the top-electrode at a different area. For this reason the top SRO layer needs to be patterned, so that there is no conduction between individual top electrodes. The structuring process, which is done by photo-lithography, is clarified by figure 8.

In the first step a photo-lithographic resist is coated on the surface. In this case a OPD-4262 photo-lithographic resist has been used, which consists of 2% tetramethylammoniumhydroxide (TMAH) solution in water. To be more precise, a photo-lithographic resist is sensible to light and it will undergo a photochemical reaction while being exposed to light of a certain wavelength. The advantage in particular is that after the photochemical reaction the material becomes resistant or susceptible to etching, depending on if it is a positive respectively a negative photo-lithographic resist. OPD-4262 is a positive photo-lithographic resist and thus protects the subjacent layers from the etching. To pattern the surface which is covered by photo-lithographic resist, a mask is used which transmits light on areas where a photochemical reaction is required and is opaque at the remaining area. Then the sample with the mask attached is exposed to white light. In the next step the SRO-top electrode is etched by Argon-beam dry-etching. The etching rate is approximately $10\,nm\,min^{-1}$ and is applied for ten minutes. Finally the remaining photo-lithographic resist is erased in a supersonic acetone bath and cleaned in a ethanol bath. Now it is possible to measure from two different top-electrodes.

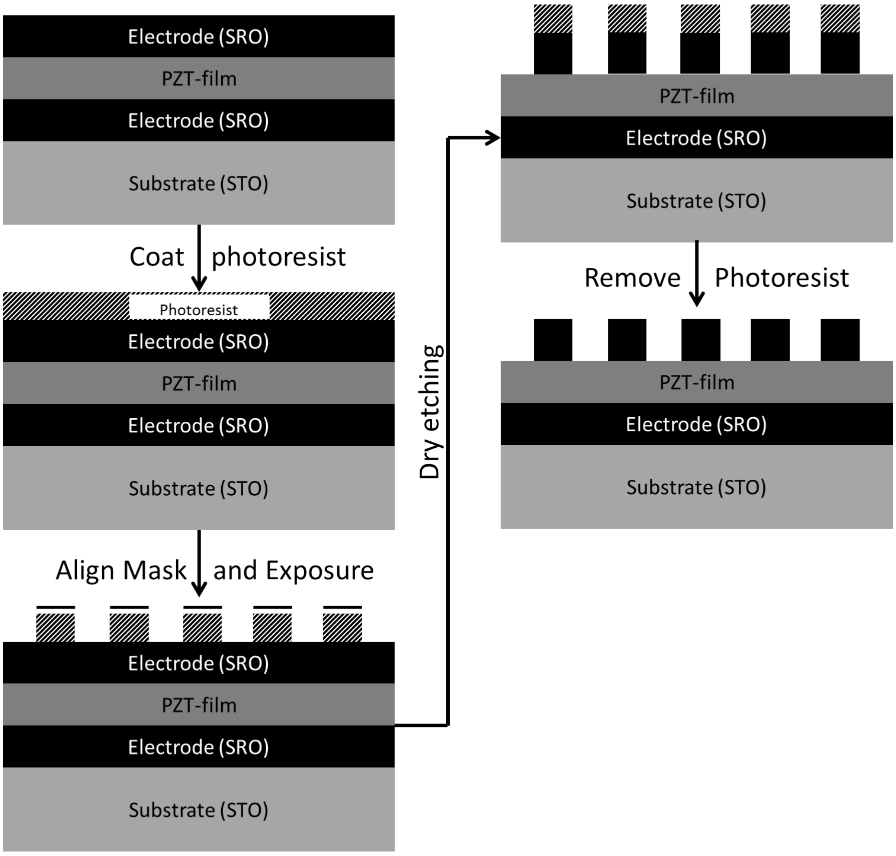

Figure 8: Schematic of photo-lithographic structuring process

3.2 Sample Characterization

This section reports on how the samples are characterized and which technologies were used therefore. At first the crystal structure of the samples were investigated by X-ray diffraction and secondly the ferroelectricity of the samples was determined by the Sawyer Tower method.

3.2.1 Crystal structure

As in section 2.1 already indicated it is important to investigate the crystal structure of the sample. For this purpose X-ray diffraction was used.

XRD

This technique irradiates X-rays of a specific wavelength at different angles on a sample. The sample bends the incident X-rays according to the model of optics and the diffracted beam can be recorded at equidistant by a detector. This leads to a specific diffraction pattern which depends on the intensity and the wavelength and consequently on the phase of the material.

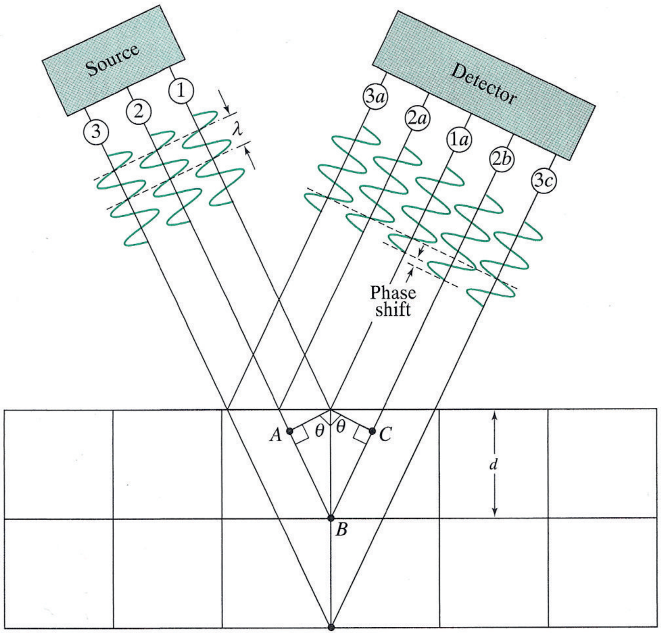

Figure 9: The emitted X-rays are reflected from parallel atomic layers and detected. Through the path-length difference between X-rays reflected from different planes interference occurs.[5]

Figure 9 shows the fundamental set-up of an XRD. The source irradiates a beam of parallel X-rays hitting the surface, which also penetrate the sample and reach deeper layers. At each atomic layer the X-rays get reflected, as a consequence the different rays interfere on there way to the detector and because of the difference of distance travelled there is also a phase shift between rays of different penetration depth. At a particular angle of incident that will cause the reflected rays to form constructive interference and by this information the distance between the atomic layers can be calculated, through Bragg's law: $2d \sin\theta = n\lambda$, with n being an integer and determines the order of the reflection, λ the wavelength of the reflected ray, θ the incident angle and d the distance between layers, and thus the crystal structure of the sample. In this study the Panalytical Xpert of Philipps has been used.

3.2.2 Ferroelectricity

The properties of ferroelectricity are determined by hysteresis loop measurements, therefore the sample response is measured whilst applying an external electric field, to be more precise a voltage difference. Owing to this the samples are structured in the shape of capacitors. The measured quantity is the current through which the polarization can be calculated by the following formula:

$$I = \frac{dQ}{dt} = A \cdot \frac{dP}{dV} \cdot \frac{dV}{dt} \tag{1}$$

To conclude, the polarization hysteresis loop of a sample can be obtained by applying a voltage to the capacitive set-up, measuring the current and using equation (1). The Sawyer Tower method is the traditional hysteresis loop measurement set-up. This circuit uses a charge measurement method which is achieved by a reference capacitor in series with the ferroelectric capacitor. Nowadays the Sawyer Tower circuit has been improved by applying a virtual ground and therefore avoiding noise. In this thesis the commercial aixACCT Analyzer TF2000 apparatus has been used to execute hysteresis loop measurements and fatigue measurements.

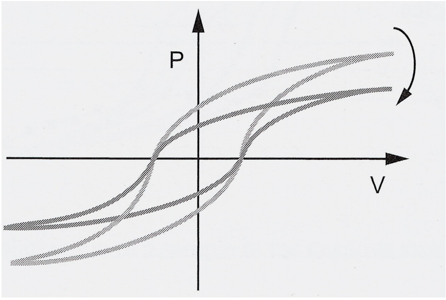

Figure 10: Flattening of hysteresis loop due to fatigue [7]

The change of the polarization hysteresis loop depending on the number of switching cycles is called Fatigue behaviour. This is important, because it has been

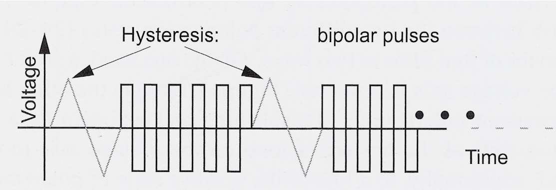

Figure 11: Triangular and bipolar fatigue excitation signal [7]

observed that the more switching occurs the more the saturation polarization decreases(figure 10). As a consequence also the remanent polarization falls and the hysteresis loop flattens. This is of great importance to ensure a long lifetime operation. The Fatigue measurement of the aixACCT Analyzer TF2000 changes between triangular pulses for hysteresis loop measurements and bipolar pulses for fatigue. The length of the bipolar pulses between the hysteresis loop measurements increase exponentially with time(figure 11). The used parameters can be find in table 3.

Parameter	Value
Waveform	triangle
Hysteresis Frequency	100 Hz
Hysteresis Amplitude	10 V
Fatigue Frequency	100 000 Hz
Fatigue Amplitude	10 V

Table 3: Fatigue and Hysteresis measurement parameters

4 Results

The results obtained from the Panalytical expert as well as the aixACCT Analyzer TF2000 will be presented in this section.

4.1 XRD measurement results

In figure 12 the 2θ-ω results for PZT compositions of PZT_1 to PZT_5 are shown. The dashed lines connecting the peaks of the different plots indicate that the reflections of same lattice parameters are similar. The first dashed line stands for the PZT{001} direction, the second one for STO(001) plane, the third one for the PZT{002} direction and the forth one for the STO(002) plane. This tells that all the samples have epitaxial growth with {001} direction. Figure 13 zooms in to only show the 2θ-ω measurements at the PZT (002) peak. The corresponding rocking curves for the peak positions of PZT(002) diffraction can be seen in figure 14. The full-width at half-maximum values can be find in table 4.

Parameter	PZT_1	PZT_2	PZT_3	PZT_4	PZT_5
Position	22.909°	23.121°	22.926°	23.002°	22.551°
FWHM	0.439°	0.402°	0.506°	0.599°	0.461°

Table 4: Position and Full-width at half-maximum intensity(FWHM) of the PZT (002) rocking curves

4.2 Ferroelectric measurement results

The polarization hysteresis loops for all used compositions can be seen in figure 15. Figure 16 shows the saturation polarization P_s and the remanent polarization P_r against the Composition. Finally, in figure 17 the coercive field strength dependent on the composition is shown.

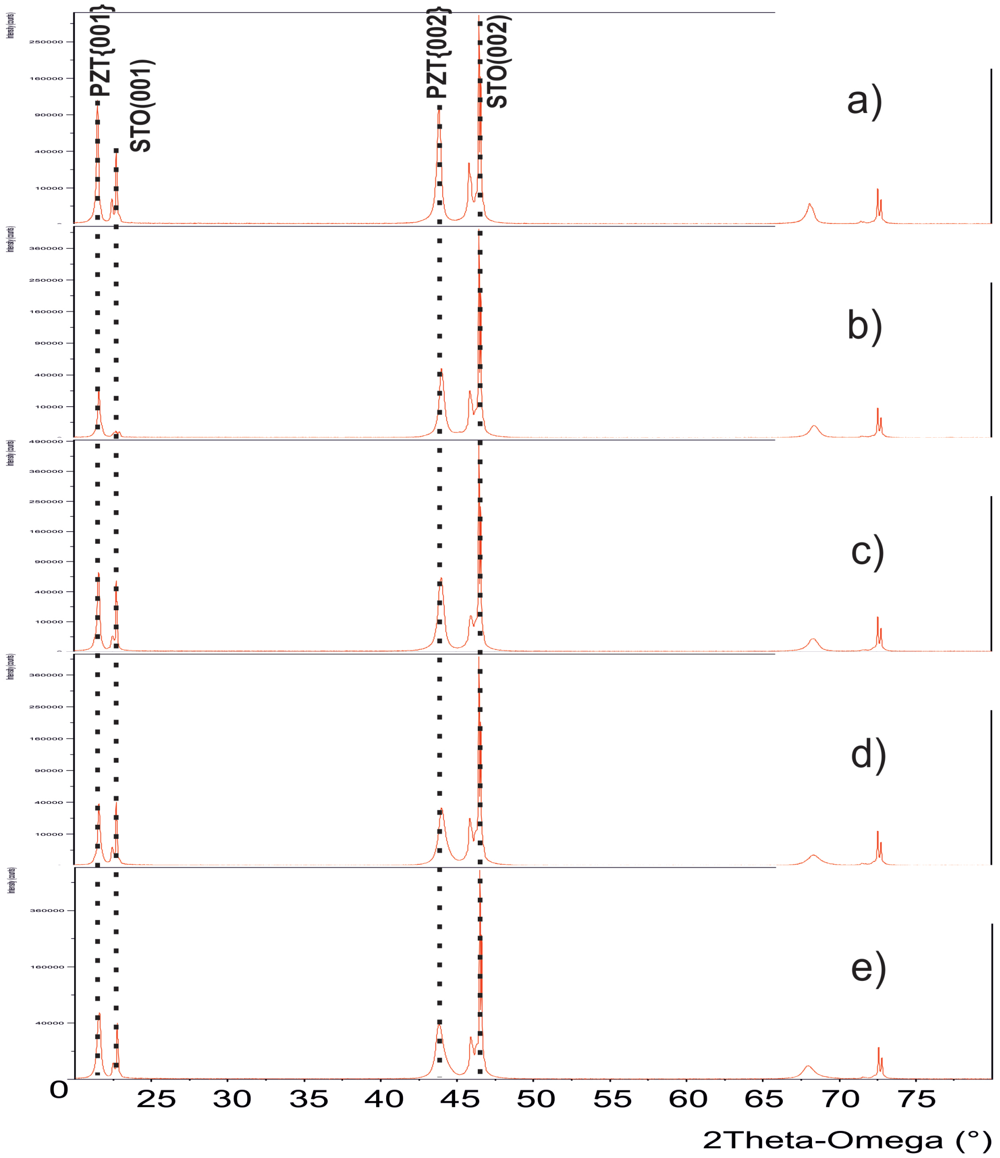

Figure 12: 2θ-ω XRD measurement for a) PZT_1 b) PZT_2 c) PZT_3 d) PZT_4 e) PZT_5

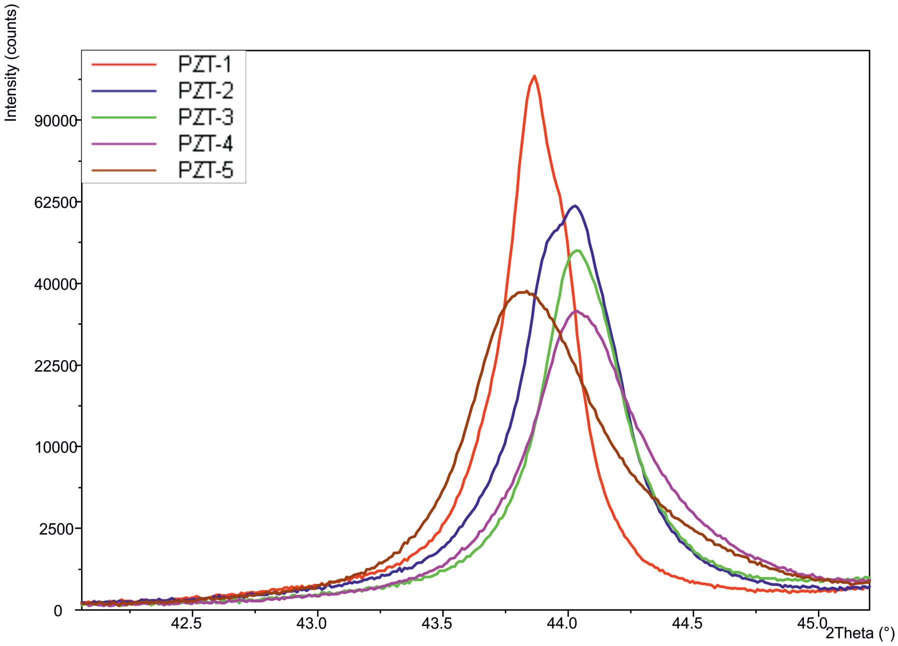

Figure 13: 2θ-ω XRD measurement at PZT (002) peak

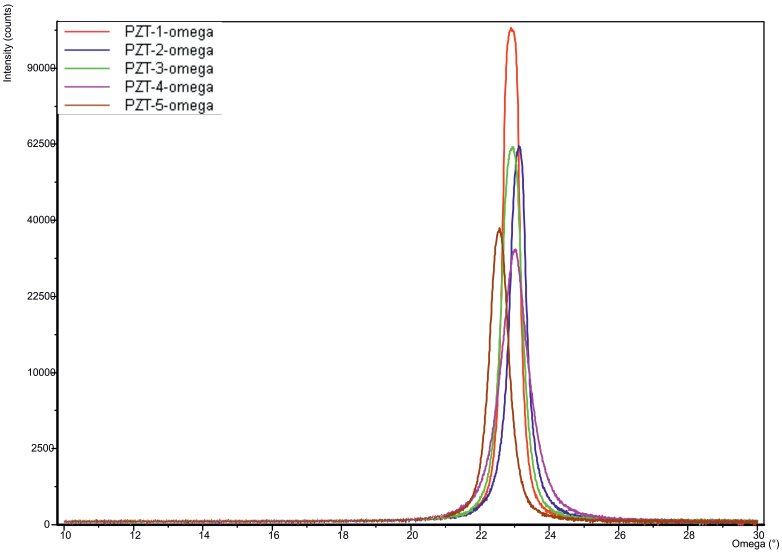

Figure 14: ω XRD measurement

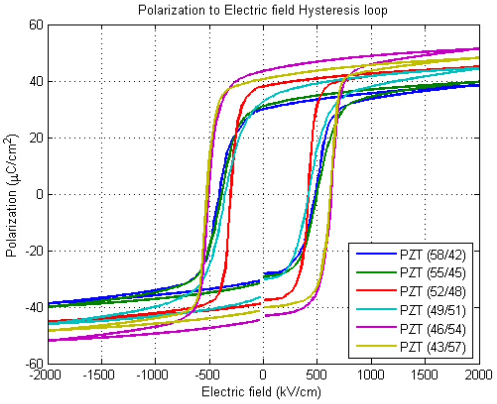

Figure 15: Polarization Hysteresis Loops

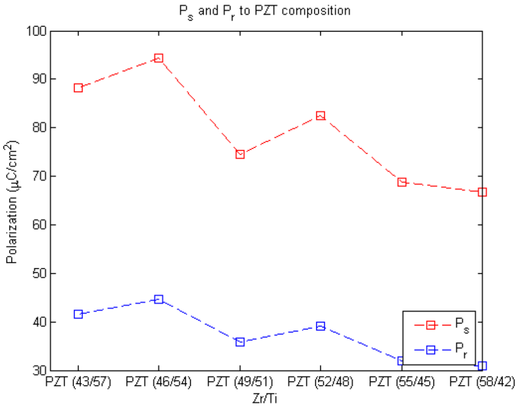

Figure 16: Saturation Polarization P_s and Remanent Polarization P_r against Composition

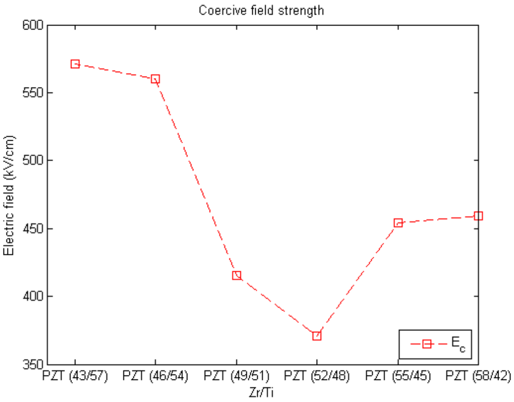

Figure 17: Coercive field strength against Composition

5 Discussion and Conclusion

First it is needed to say that initially five fabricated samples were not showing any good measuring results and it was not possible to bring the cause to light. In order to get results the samples were fabricated cautious again, providing good results. Overall this shows that small mistakes can be of great impact and that error ranges can vary quite heavily.

About the sample fabrication is to conclude that the films were grown with high epitaxy, what is indicated by the low full-width at half-maximum (FWHM) values, which reach maximum 0.6°. Next, the 2θ-ω measurementsfigure 12 lead to the assumption that the growth occurred in the $\{001\}$ direction as expected, due to the alignment with the substrate. If a closer look is taken at the 2θ-ω measurement at the PZT $\{002\}$ direction peak (figure 13) it is observed that the angle of the peaks differ, consequently also the lattice parameter differs, according to Bragg's law. This is comparable to bulk PZT where the volume differs around the MPB

The polarization hysteresis loops look like expected. For higher Zirconate fraction the loops look less flat and more rounder shaped. Furthermore, the saturation polarization P_s, the remanent polarizationP_r and the coercive field strength E_c values are lower. This indicates a less ferroelectric behaviour, what is reasonable because this point into the direction of bulk $PbZrO_3$ which is not ferroelectric as well. On the other side with high Titanate fraction, the loops are more rectangular shaped and also posses high P_s, P_r and E_c values, which indicate a strong ferroelectric behaviour. Also here this is pointing to the bulk counterpart $PbTiO_3$, which is highly ferroelectric. For the compositions near the morphotropic phase boundary the saturation and remanent polarization have a local minimum and the coercive field strength even shows a total minimum. This is in accordance to the expectations that near the morphotropic phase boundary a polarization switch is more easily achieved.

References

[1] Enerdata Publication. *World energy use in 2010: over 5% growth.* 2011.

[2] E.A. and Neppiras. "Piezoelectric ceramics 1971: B. Jaffe, W. R. Cook Jr and H. Jaffe. London and New York: Academic Press. 317 pp." In: *Journal of Sound and Vibration* 20.4 (1972), pp. 562 –563. ISSN: 0022-460X. DOI: `10.1016/0022-460X(72)90684-0`. URL: `http://www.sciencedirect.com/science/article/pii/0022460X72906840`.

[3] K.M. Rabe, C.H. Ahn, and J.M. Triscone. *Physics of ferroelectrics: a modern perspective.* Vol. 105. Springer Verlag, 2007.

[4] University of Cambridge. *DoITPoMS -> TLP Libary -> Piezoelectric Materials -> PZT.* [Online; accessed 18-March-2012]. 2012. URL: `\url{http://www.doitpoms.ac.uk/tlplib/piezoelectrics/pzt.php}`.

[5] J.P. Schaffer et al. *The science and design of engineering materials.* Irwin, 1995.

[6] Wikipedia. *Ferroelectricity — Wikipedia, The Free Encyclopedia.* [Online; accessed 22-March-2012]. 2012. URL: `\url{http://en.wikipedia.org/w/index.php?title=Ferroelectricity&oldid=483331604}`.

[7] R. Waser, U. Böttger, and S. Tiedke. *Polar oxides: properties, characterization, and imaging.* Vch Verlagsgesellschaft Mbh, 2005.

[8] Wenwu Cao and L. Eric Cross. "Theoretical model for the morphotropic phase boundary in lead zirconate–lead titanate solid solution". In: *Phys. Rev. B* 47 (9 1993), pp. 4825–4830. DOI: `10.1103/PhysRevB.47.4825`. URL: `http://link.aps.org/doi/10.1103/PhysRevB.47.4825`.

[9] Wikipedia. *Pulsed laser deposition — Wikipedia, The Free Encyclopedia.* [Online; accessed 2-March-2012]. 2012. URL: `\url{http://en.wikipedia.org/w/index.php?title=Pulsed_laser_deposition&oldid=474712344}`.

[10] D.A. Glocker et al. *Handbook of thin film process technology.* Vol. 1. Institute of Physics Publishing, 1995.

[11] P.M. Riele. “Direct patterning of oxides by pulsed laser stencil deposition”. PhD thesis. 2008.

[12] R. Ramesh and DG Schlom. “Orienting ferroelectric films”. In: *Science* 296.5575 (2002), pp. 1975–1976.

[13] JH Kim et al. “Microstructural and ferroelectric properties of a chemical solution deposited epitaxial $PbZr_{0.5}Ti_{0.5}O_3$ thin film on a $SrRuO_3/SrTiO_3$ substrate”. In: *Journal of materials research* 14.4 (1999), pp. 1190–1193.

[14] R. Eason. *Pulsed laser deposition of thin films: applications-led growth of functional materials*. Wiley-Blackwell, 2007.